

Comparison of benzil and trifluoromethyl ketone (TFK)-mediated carboxylesterase inhibition using classical and 3-D quantitative structure activity relationship analysis

Toshiyuki Harada^{a, †}, Yoshiaki Nakagawa^{a, †}, Randy M. Wadkins^b, Philip M. Potter^c, Craig E. Wheelock^{d,*}

^aDivision of Applied Life Sciences, Graduate School of Agriculture, Kyoto University, Kyoto 606-8502, Japan

^bDepartment of Chemistry and Biochemistry, University of Mississippi, University, MS 38677, USA

^cDepartment of Molecular Pharmacology, St. Jude Children's Research Hospital, Memphis, TN 38105, USA

^dDivision of Physiological Chemistry II, Department of Medical Biochemistry and Biophysics, Scheeles väg 2, Karolinska Institutet, 171 77 Stockholm, Sweden

[†] These authors contributed equally to this manuscript

* Corresponding author.

Craig Wheelock

Tel.: +46-8-5248-7630

Fax: +46-8-736-0439

Email: craig.wheelock@ki.se

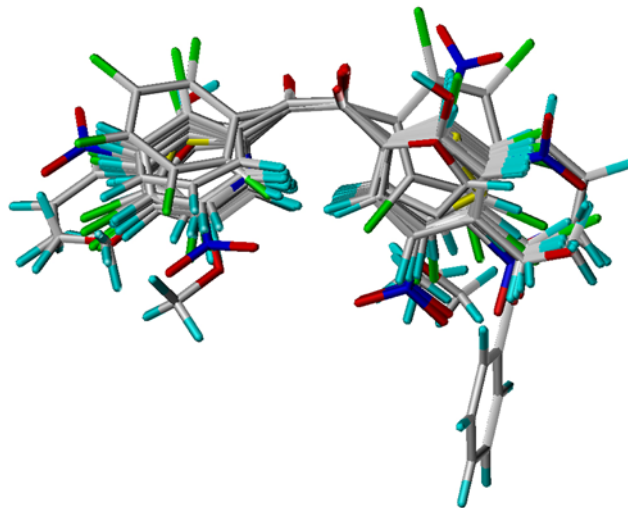


Figure S1. Superposition of all 32 benzil-analogs used to generate the CoMFA models.

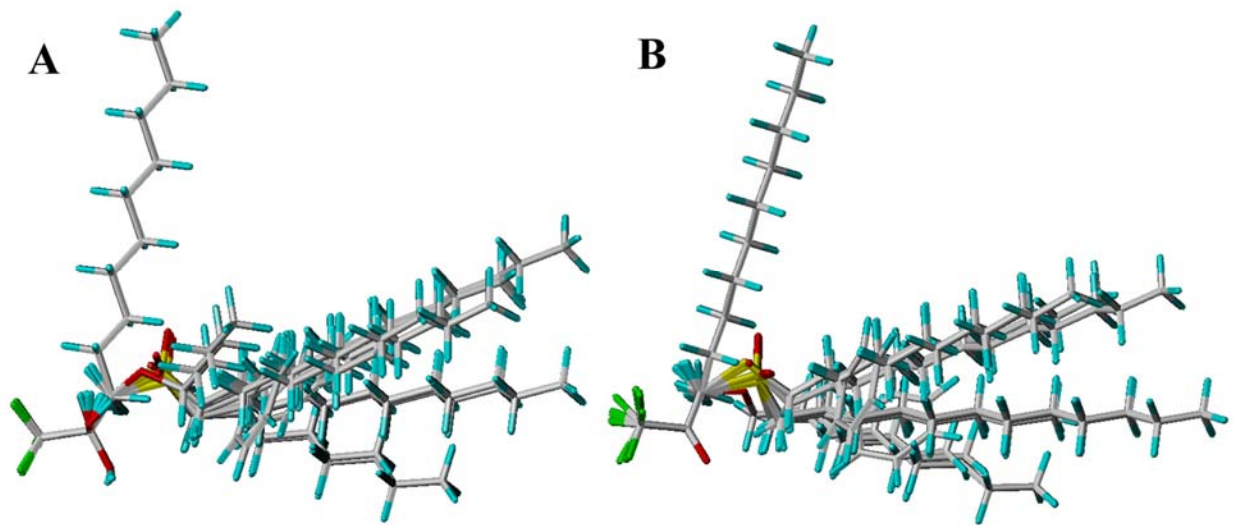
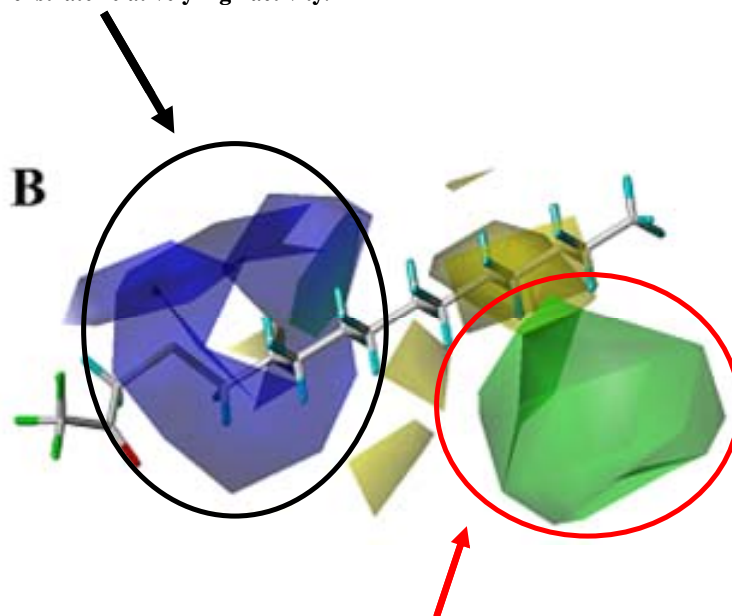


Figure S2. Superposition of TFKs in *gem*-diol (A) and ketone (B) geometries with all 17 TFK compounds.

The alkyl moiety of -S- containing compounds (33, 36, 40, 43, 47, 48) go through this ring. These compounds demonstrate relatively high activity.



The alkyl moiety of $-(=O)S(=O)-$ containing long chain TFK compounds (35, 38) reach the green region. These compounds show relatively high activity.

Figure S3. CoMFA map for the hiCE model with the TFK inhibitor in the ketone form. Specific areas of enhanced activity are described on the map.

The alkyl moiety of the $-CH_2-$ containing compound (39) goes through this ring.
This compound demonstrate relatively high activity.

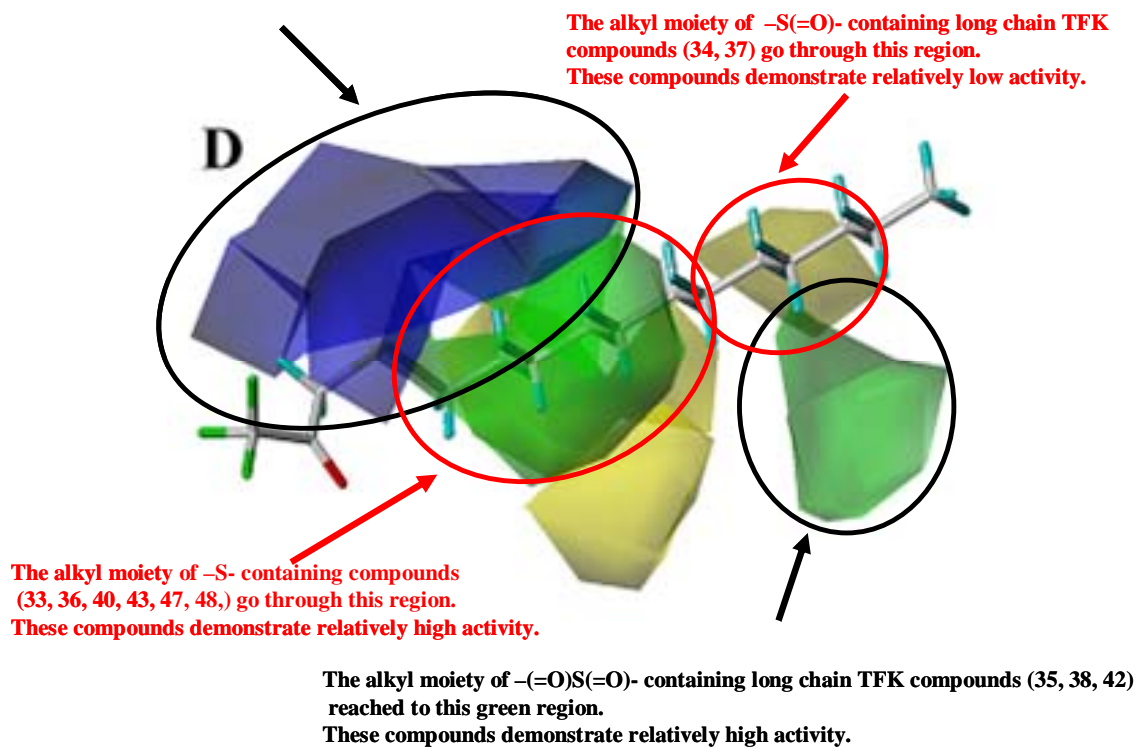
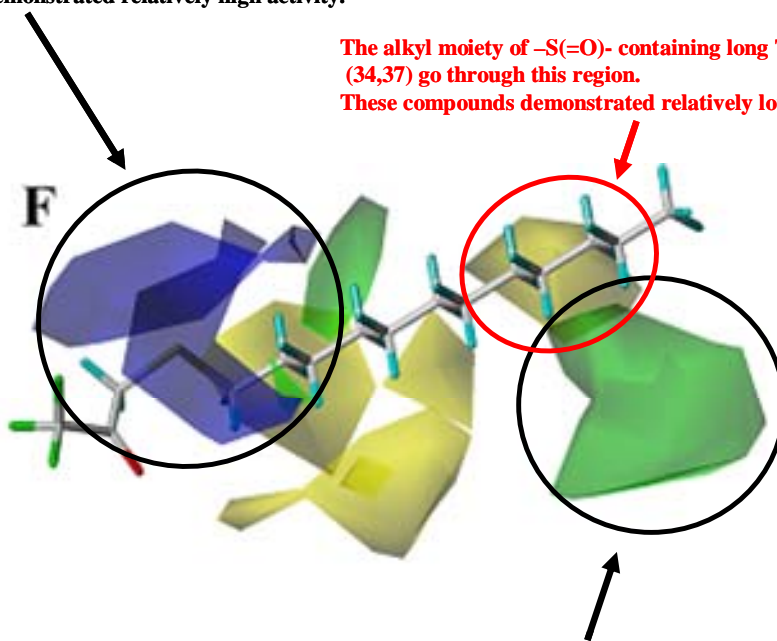


Figure S4. CoMFA map for the hCE1 model with the TFK inhibitor in the ketone form. Specific areas of enhanced activity are described on the map.

The alkyl moiety of the $-CH_2-$ containing compound (39) goes through this region.
This compound demonstrated relatively high activity.

The alkyl moiety of $-S(=O)-$ containing long TFK compounds (34,37) go through this region.
These compounds demonstrated relatively low activity.



The alkyl moiety of $-(=O)S(=O)-$ containing long TFK compounds (35, 38) reached to this green region.
These compounds demonstrated relatively high activity.

Figure S5. CoMFA map for the rCE model with the TFK inhibitor in the ketone form. Specific areas of enhanced activity are described on the map.

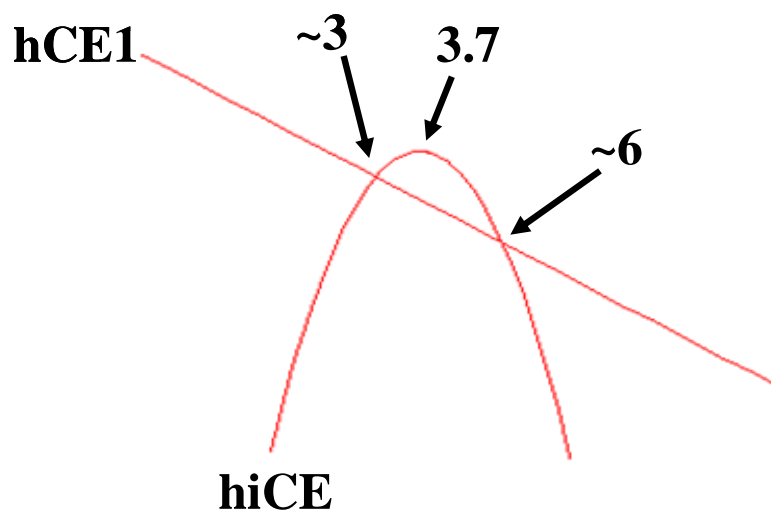


Figure S6. Graphs of the classical QSAR equations for the benzil-analogs displaying the volume dependence of hCE1 and hiCE (Eq. 1 and Eq. 2). To make the graphs, a distinct assumption was made that the log P term is constant (however, it ranges from -3.2 to 7.2). Accordingly, each equation was changed to the corresponding quadric equation using this hypothesis and graphed using GCalcPlus (ver. 2.03), with the resulting equations shown below:

$$pK_i = -1.79 \text{ vol}^2 + 13.2 \text{ vol} + 17.0 \quad (\text{Eq. 1}')$$

$$pK_i = -0.883 \text{ vol} + c \quad (\text{Eq. 2}')$$

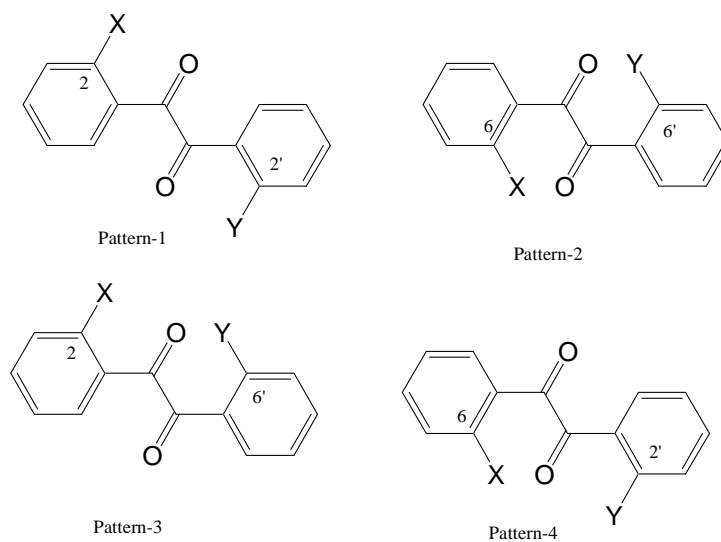


Figure S7. The four conformer patterns tested to determine the most stable conformation for construction of the superposition for the CoMFA model. Pattern 1 was selected as the template for model construction, even though the difference between Pattern 1 and 3 was only 4 kcal/mol with respect to the enthalpy of formation (ΔH).

Table S1. Experimental and predicted pK_i values and associated physicochemical parameters for all compounds based upon the mixed benzil-analog and TFK inhibitor CoMFA analysis.

N°	Observed			log P	log P ²	vol	vol ²	Predicted		
	hiCE	hCE1	rCE					hiCE	hCE1	rCE
1	7.83	7.35	6.99	3.38	11.42	3.33	11.07	7.02	6.72	6.52
2	6.78	6.64	6.40	3.76	14.14	3.49	12.15	6.94	6.66	7.02
3	6.97	6.74	8.02	4.90	24.01	3.69	13.61	7.33	6.93	8.02
4	6.45	5.78	6.66	4.90	24.01	3.61	13.01	6.58	6.09	6.33
5	7.63	7.13	7.76	4.06	16.48	3.63	13.18	6.95	6.49	7.62
6	6.59	6.43	7.32	4.07	16.56	3.77	14.22	6.79	6.38	7.83
7	7.15	6.28	7.19	3.39	11.49	3.26	10.64	7.18	6.83	7.43
8	7.74	7.32	7.62	4.17	17.39	3.33	11.07	7.58	7.04	7.25
9	7.64	6.80	7.79	4.67	21.81	3.72	13.83	7.60	6.61	7.25
10	7.48	6.90	6.92	3.88	15.05	3.32	11.05	7.66	6.81	6.89
11	7.22	6.27	7.30	4.38	19.18	3.79	14.33	7.51	6.54	7.24
12	8.39	7.00	6.97	4.33	18.75	3.32	11.01	8.07	6.95	7.21
13	7.99	6.76	6.70	3.60	12.96	3.34	11.15	7.79	6.60	6.84
14	7.15	5.47	6.24	3.61	13.03	4.08	16.63	7.34	5.89	7.00
15	6.86	5.81	7.14	3.61	13.03	4.05	16.41	7.22	5.60	6.90
16	8.05	5.48	7.44	4.04	16.32	3.71	13.75	8.27	6.25	7.50
17	7.67	7.11	7.82	4.16	17.31	3.30	10.92	7.57	7.09	7.78
18	-	-	8.06	-1.38	1.90	4.39	19.28	7.96	4.96	8.19
19	8.10	6.53	7.92	0.59	0.35	3.32	11.02	8.31	6.33	7.85
20	7.51	6.67	7.66	0.09	0.01	3.31	10.99	7.32	6.77	7.71
21	6.68	-	6.28	-3.20	10.24	3.28	10.77	6.67	5.72	6.42
22	6.40	4.74	6.57	-3.20	10.24	4.00	15.99	6.33	4.59	6.05
23	7.14	-	7.27	4.68	21.90	4.02	16.19	7.32	6.32	7.31
24	6.42	5.77	6.08	7.20	51.84	3.96	15.71	5.92	5.86	6.84
25	8.25	8.10	8.21	4.89	23.91	3.29	10.80	8.07	8.26	8.62
26	5.98	6.67	6.06	2.84	8.07	2.92	8.55	6.28	7.03	6.98
27	5.18	6.44	5.62	2.84	8.07	2.86	8.19	5.60	6.83	5.60
28	7.24	7.52	8.66	4.61	21.25	3.47	12.04	6.75	7.18	7.97
29	6.63	6.68	8.15	4.61	21.25	3.45	11.91	6.72	7.10	7.62
30	5.10	5.93	5.07	1.24	1.54	2.66	7.09	5.55	6.28	5.32
31	6.82	6.90	6.32	0.90	0.81	3.17	10.04	6.90	6.25	5.95
32	7.07	6.59	8.98	5.73	32.83	4.59	21.11	7.05	6.23	8.75
33	7.82	7.15	6.80	6.63	43.96	2.02	4.07	7.57	7.18	6.98
34	7.27	5.72	5.96	5.12	26.21	2.01	4.05	6.88	5.42	5.69

35	7.49	6.13	6.82	5.04	25.40	2.02	4.07	7.67	6.07	6.62
36	6.82	6.89	6.80	5.57	31.02	2.02	4.06	7.01	6.92	6.80
37	5.72	5.28	5.60	4.06	16.48	2.02	4.06	6.13	5.26	5.54
38	7.10	6.10	6.66	3.98	15.84	2.01	4.05	6.97	5.82	6.26
39	7.66	6.82	6.85	5.11	26.11	2.01	4.03	8.02	6.98	6.70
40	6.66	6.72	6.82	4.51	20.34	2.02	4.07	6.60	6.69	6.63
41	5.62	4.83	5.31	3.00	9.00	2.01	4.03	5.21	4.84	5.15
42	5.33	5.82	5.32	2.92	8.53	2.01	4.05	5.65	5.52	5.70
43	6.25	6.48	6.60	3.46	11.97	2.02	4.06	6.14	6.42	6.39
44	4.17	4.10	4.64	1.95	3.80	2.01	4.03	4.50	4.61	4.86
45	4.56	5.01	4.82	1.87	3.50	2.01	4.03	4.75	5.26	5.32
46	5.04	5.48	5.57	2.76	7.62	2.02	4.07	4.71	5.46	5.39
47	5.77	6.10	6.38	2.40	5.76	2.02	4.07	5.79	6.12	6.10
48	6.12	6.92	6.39	2.91	8.47	2.02	4.07	5.91	6.39	6.32
49	4.29	4.86	4.87	1.32	1.74	2.01	4.04	4.14	5.09	5.17
